Biochemical and Biophysical Research Communications 391 (2010) 370–375

Contents lists available at ScienceDirect

Biochemical and Biophysical Research Communications

journal homepage: www.elsevier.com/locate/ybbrc

NMR characterization of a 264-residue hyperthermostable endo-β-1,3-glucanase

Johannes H. Ippel [a,1,3], Sotirios Koutsopoulos [b,2,3], Sanne M. Nabuurs [a], Willem J.H. van Berkel [a], John van der Oost [b], Carlo P.M. van Mierlo [a,*]

[a] Laboratory of Biochemistry, Wageningen University, Dreijenlaan 3, 6703 HA Wageningen, The Netherlands
[b] Laboratory of Microbiology, Wageningen University, Dreijenplein 10, 6703 HB Wageningen, The Netherlands

ARTICLE INFO

Article history:
Received 27 October 2009
Available online 12 November 2009

Keywords:
Protein
Glycoside hydrolase
Laminarin
Endo-β-1,3-glucanase
Calorimetry

ABSTRACT

Insight into the hyperthermostable endo-β-1,3-glucanase *pf*LamA from *Pyrococcus furiosus* is obtained by using NMR spectroscopy. *pf*LamA functions optimally at 104 °C and recently the X-ray structure of pfLamA has been obtained at 20 °C, a temperature at which the enzyme is inactive. In this study, near-complete (>99%) NMR assignments are presented of chemical shifts of *pf*LamA in presence and absence of calcium at 62 °C, a temperature at which the enzyme is biologically active. The protein contains calcium and the effects of calcium on the protein are assessed. Calcium binding results in relatively small chemical shift changes in a region distant from the active site of *pf*LamA and thus causes only minor conformational modifications. Removal of calcium does not significantly alter the denaturation temperature of *pf*LamA, implying that calcium does not stabilize the enzyme against global unfolding. The data obtained form the basis for elucidation of the molecular origins involved in conformational stability and biological activity of hyperthermophilic endo-β-1,3-glucanases at extreme temperatures.

Introduction

Hyperthermophilic microorganisms flourish in extreme environments of conditions that were until recently considered as incompatible with life. *Pyrococcus furiosus* is an anaerobic hyperthermophile, which was discovered in geothermally heated marine sediments at temperatures exceeding 100 °C [1]. The organism contains a large collection of hyperthermostable enzymes that have potential for applications in biotechnology and industrial biocatalysis [2]. One of these enzymes is the extracellular *pf*LamA, of which several properties have been characterized [3]. *pf*LamA belongs to the class of laminarases (EC 3.2.1.39) of the glycoside hydrolase family GH-16 [4]. The enzyme hydrolyzes 1,3-β-D-glucosidic linkages in 1,3-beta-D-glucans, e.g. laminarins, curdlans, paramylons, and pachymans. *pf*LamA is optimally active at 104 °C, a condition where proteins from mesophilic organisms rapidly denature, whereas it is inactive at room temperature [5,6].

The crystal structure of *pf*LamA at 2.16 Å resolution has been recently elucidated (PDB entry 2VY0) [7]. In general, protein structures belonging to the GH-16 family have a beta jelly-roll fold with a highly concave side to which a glycan polymer substrate binds and contain at least one metal-binding site [8]. Indeed, X-ray structural analysis shows that *pf*LamA contains one calcium ion, which is located opposite to the active site of the enzyme (Fig. 1). The dissociation constant of the enzyme-calcium complex is 30 nM at 20 °C [9]. Catalytic residues E170, D172, and E175 of *pf*LamA are involved in hydrolysis of the 1,3-β-glycosidic bond and are highly conserved in the GH-16 family [8]. These three amino acids are located in a single β-strand and their side chains point towards the substrate-binding pocket. Mutation of either one of the aforementioned two glutamate residues abolishes enzymatic activity almost completely.

Currently, virtually all three-dimensional structures of hyperthermostable proteins have been obtained using crystallography, as is the case for *pf*LamA. X-ray data are extracted from protein crystals at temperatures far lower than the normal operating temperature of the proteins involved. Although supported by little experimental data, it is generally believed that protein crystals grown at ambient temperatures are imperfect proxies for the conformational properties of hyperthermostable proteins that are active at temperatures above 100 °C [10]. NMR spectroscopy is a suitable technique to solve the three-dimensional structure of a protein in solution at temperatures well above room temperature. Most solution structures of thermo- and hyperthermostable proteins have been derived from data obtained at temperatures

Abbreviations: *pf*LamA, endo-β-1,3-glucanase from *Pyrococcus furiosus*; NMR, nuclear magnetic resonance; NOESY, nuclear Overhauser effect spectroscopy; HSQC, heteronuclear single quantum correlation; DSC, differential scanning calorimetry.

* Corresponding author. Fax: +31 317 484801.
E-mail address: carlo.vanmierlo@wur.nl (C.P.M. van Mierlo).
[1] Present address: NMR Spectroscopy Research Group, Bijvoet Center for Biomolecular Research, Utrecht University, Padualaan 8, 3584 CH Utrecht, The Netherlands.
[2] Present address: Massachusetts Institute of Technology, 77 Massachusetts Av., Center for Biomedical Engineering NE47–307, Cambridge, MA 02139, USA.
[3] These authors contributed equally to this work.

0006-291X/$ - see front matter © 2009 Elsevier Inc. All rights reserved.
doi:10.1016/j.bbrc.2009.11.065

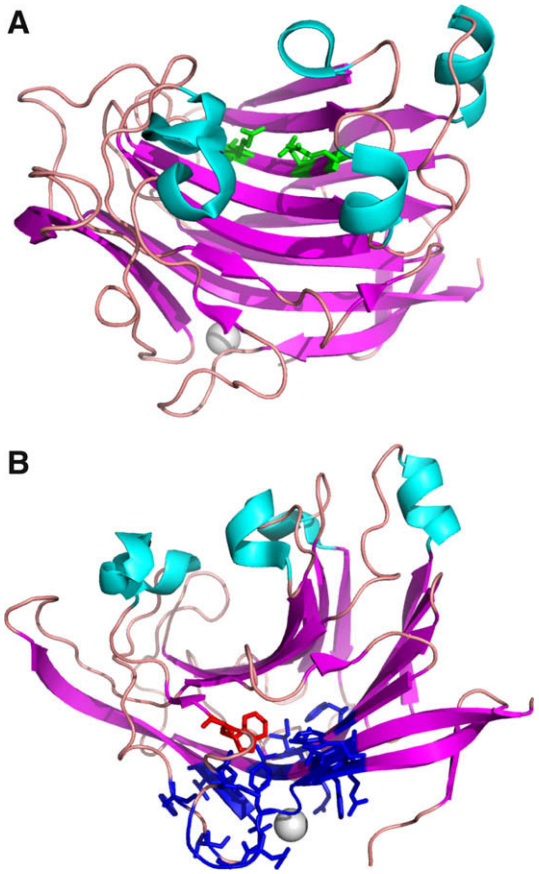

Fig. 1. Cartoon drawings of *pf*LamA, with calcium shown as gray sphere. Beta sheets and alpha-helices are colored magenta and cyan, respectively. (A) Top view of *pf*LamA with E170, D172, and E175, involved in substrate binding, colored green. (B) Side view of *pf*LamA with amino acids that are identified by NMR spectroscopy to be affected by Ca^{2+} binding colored blue; W64, located near the active site of *pf*LamA, is also affected by calcium binding (see Fig. 3) and is highlighted in red.

between room temperature and 40 °C. Only five solution structures have been deduced from NMR data obtained at 50–65 °C, all of small, less than 100 residues-containing proteins [11–15].

With this work we aim to elucidate the molecular origins involved in conformational stability and biologically activity of the 264-residue hyperthermophilic *pf*LamA from *P. furiosus* at extreme temperatures. Currently, for no (hyperthermostable) glucanase NMR assignments are available and thus no solution structures of these proteins are known. To understand the (sub)molecular properties of hyperthermostable endo-β-1,3-glucanases, we aim to solve the solution structure of *pf*LamA in its catalytically active state at elevated temperatures. The latter is considered important, as the X-ray structure of *pf*LamA has been obtained at 20 °C, a temperature at which the protein is biologically inactive. The data presented here of *pf*LamA at 62 °C reveal insight into the role of Ca^{2+} in *pf*LamA's conformational characteristics and form the basis for elucidation of its solution structure.

Materials and methods

Protein expression and purification. The sequence of the *pf*LamA gene has been deposited in the GenBank™ database (Accession No. AF013169). Residues 34–297 of *pf*LamA were expressed in transformed *E. coli* BL21 (DE3) cells using the T7 expression system, as described elsewhere [3]. Cells were grown at 37 °C in M9 minimal medium containing $^{15}NH_4Cl$ and ^{13}C-glucose. The M9 medium was supplemented with 2 mM $MgSO_4$, 0.1 mM $CaCl_2$, and 10 μM $FeCl_3$, and contained thiamin, biotin, and kanamycin. After expression of *pf*LamA, the cells were centrifuged at 4 °C, resuspended in Tris buffer and lysed by sonication. Purification involved heat incubation of the cell extract at 85 °C for 45 min to denature the non-hyperthermostable proteins of *E. coli*; protein aggregates were removed by centrifugation. Further purification of the *pf*LamA-containing supernatant was performed using a phenyl-Sepharose and a Superdex 200 column (Amersham Pharmacia, Sweden).

NMR samples of 1.5 mM uniformly [^{13}C, ^{15}N]-labeled *pf*LamA were prepared in 10 mM sodium phosphate, pH 7.0, with 10% D_2O (Cambridge Isotope Laboratory, Cambridge, MA), 100 μM of 2,2-dimethyl-2-silapentane-5-sulfonic acid (DSS), and 0.01% (w/v) azide. Samples were stored at 4 °C; under these conditions *pf*LamA was stable for at least four years.

Mass spectrometry. Matrix-assisted laser desorption/ionization time-of-flight mass spectrometry (MALDI-TOF, Voyager DE-RP, PerSeptive Biosystems, Framingham, MA, USA) and size exclusion chromatography showed that the 264-residue *pf*LamA in solution is a monomer.

Trypsinized *pf*LamA was characterized by electrospray ionization-quadrupole-time-of-flight (ESI-Q-TOF) mass spectrometry. Separation of the *pf*LamA peptide fragments was performed using a Zorbax 300 Extend-C18 column (Agilent Technologies, Palo Alto, CA) and an Agilent 1200 series chromatography system coupled to Agilent 6510 Q-TOF; spray voltage of 3.8 kV, gas temperature of 275 °C, nebulizer gas at 10 psi, and a drying gas of 4 l/min were used. Positive ion data-dependent acquisition range in the scan mode was 100–1799 *m/z* and for the MS/MS mode 100–2000 *m/z*. The charge priority of MS/MS acquisition was +2 (charges), +3, >+3, unknown, +1. Data were collected and analyzed using the Agilent MassHunter software (Agilent, Technologies, Palo Alto, CA). Peptide identification and assignment of possible amino acid chemical modifications was confirmed by inspection of the MS/MS spectra and by using the ProteinProspector software (http://prospector.ucsf.edu/).

NMR spectroscopy. Two sets of spectra were collected for *pf*LamA: one set was obtained using a sample in which half of the *pf*LamA molecules had their calcium-binding site filled with Ca^{2+}. The other set was obtained using a sample in which all *pf*LamA molecules had their calcium-binding site filled with Ca^{2+} (achieved by adding $CaCl_2$ to the sample to a final concentration of approximately 10 mM). Preliminary titration and back-titration NMR experiments were performed with increasing $CaCl_2$ and EDTA concentrations, respectively prior to determining the optimal conditions for the study.

NMR data were acquired on Bruker AMX500, DRX700, and DRX900 spectrometers, equipped with triple-resonance probes with *z*-gradients. ^1H–^{15}N HSQC, ^1H–^{13}C HSQC, 3D-^{15}N-edited NOESY, 3D-^{13}C-edited NOESY and CBCA(CO)NH, HNCACB, HNCO, HN(CA)CO, HBHA(CO)NH, HN(CO)CA, and HCCH-TOCSY triple-resonance experiments were collected to complete ^1H, ^{13}C, and ^{15}N resonance assignments of calcium-containing and no calcium-containing *pf*LamA molecules. To assign side-chain resonances of tryptophans, 2D-TOCSY and 2D-NOESY spectra were collected on unlabeled samples of *pf*LamA.

All NMR data were processed with Xwinnmr (Bruker, Rheinstetten, Germany) and analyzed with CARA v1.5.5/NEASY (Institute of Molecular Biology and Biophysics, ETH Zürich, Switzerland) and Sparky (TD Goddard and DG Kneller, University of California, San Francisco, USA).

Differential scanning calorimetry. Calorimetric studies were carried out in a VP-DSC calorimeter (MicroCal Inc., Northampton, MA). The effect of calcium ions on thermal stability of *pf*LamA was investigated through addition of 1 mM $CaCl_2$ or 1 mM EDTA to the protein solution. Heat exchanges of non-labeled *pf*LamA

were recorded between 20 and 130 °C using as reference the appropriate buffer solution (i.e., with or without 1 mM $CaCl_2$, or with 1 mM EDTA). Samples were degassed under vacuum for 15 min prior to loading the cells, which were maintained under 2.5 bar pressure to avoid boiling of the sample. The concentration of *pf*LamA was 7.6 μM in 10 mM sodium phosphate, pH 7.0.

Heat exchanges of *pf*LamA were also studied using protein concentrations ranging between 0.1 and 2.0 mg/mL which led to the same heat capacity values when the data were normalized to the protein concentration used. The temperature increased at a rate of 30 °C/h. Heat exchanges of *pf*LamA were also recorded using heating rates between 6 and 90 °C/h, which led to similar results.

DSC data were analyzed using Origin software (MicroCal Inc.). Thermograms of *pf*LamA with 1 mM $CaCl_2$ were smoothed using the Origin 5-point adjacent averaging algorithm. This smoothing was necessary, as addition of $CaCl_2$ to the phosphate containing *pf*LamA solution leads to formation of calcium phosphate salts, causing increased noise of DSC thermograms. Precipitation of these salts results in Ca^{2+} sequestration. To determine the concentration of free calcium interacting with *pf*LamA we used a computational approach [16] in which the proton dissociation, ion-pair formation constants, and solubility products for calcium phosphate salts (i.e., hydroxyapatite, octacalcium phosphate, tricalcium phosphate, and dicalcium phosphate dihydrate) are taken into account. [17–21] The calculations reveal that in the temperature range of 20–45 °C the concentration of free Ca^{2+} interacting with *pf*LamA is approximately 0.5 mM (i.e., 60-fold higher than the concentration of *pf*LamA). Increasing temperature to 120 °C results in higher concentrations of free Ca^{2+}, because the sparingly soluble salts octacalcium phosphate and hydroxyapatite are more soluble at elevated temperatures [17].

Results and discussion

Mass spectrometric analysis of pfLamA

Based on the amino acid sequence of *pf*LamA, the theoretical isotopically-averaged molecular mass of *pf*lamA is 30,085 Da [3]. MALDI-TOF analysis of a non-labeled protein sample yields a value of 30,135 Da. The difference in molecular masses suggests that *pf*LamA in solution may contain a calcium ion and furthermore that a post-translational modification occurred.

To test whether methionine oxidation occurs, trypsinized *pf*LamA peptide fragments were separated by HPLC and subsequently analyzed by ESI-Q-TOF mass spectrometry. Trypsin cleaves *pf*LamA at the carboxyl side of residue K44. It turns out that M34 is indeed present in both the oxidized and non-oxidized form in the ensemble of *pf*LamA molecules (Fig. 2). This oxidation of *pf*LamA has not been reported previously. Further analysis of the data shows that in a fraction of *pf*LamA molecules M34 is cleaved from the protein.

Quantitative analysis using combined peak integration of the extracted chromatograms for all charged states reveals that M34 is oxidized in approximately 10% of *pf*LamA molecules, whereas 12% of *pf*LamA molecules are devoid of M34 (Fig. 2). Furthermore, we observe deamidation of N60 in 30% of the *pf*LamA molecules (potentially, deamidation of Q45 instead of N60 is also possible, although less likely). Fragment 105–128 of *pf*LamA turns out to be phosphorylated. However, as this fragment contains two serines, two threonines, and one tyrosine, we cannot yet resolve which of these residues is phosphorylated.

Assignment of chemical shifts of pfLamA

Practical considerations led us to select 62 °C as the temperature to perform NMR experiments. Excellent quality, high-resolution 1D and 2D NMR spectra of *pf*LamA are recorded at temperatures up to 95 °C. However, according to hardware specifications, 62 °C is approximately the maximum temperature a sample can be for long periods of time inside a triple-resonance probe, without risking damage to construction materials of the probe.

Elevated temperatures may lead to instability of NMR samples due to turbulence and refluxing of heated water. Therefore, we prepared samples in standard 5 mm NMR tubes capped with a sterilized Teflon plug, positioned just above sample volume. A tiny hole in the plug prevents build up of pressure, and allows for a slow and controlled release of water vapor from the sample. The plug prevents water droplets, which condense on the glass in the top part of the NMR tube, to slide back into the sample. Consequently, sudden changes in homogeneity of the protein solution are avoided. The original starting situation can easily be recovered after recording a three-dimensional NMR spectrum through centrifugation of the NMR tube.

Two sets of assignments of *pf*LamA are deposited in BioMagResBank (www.bmrb.wisc.edu) (Accession No. BMRB-16481). Amino acid residues that are in proximity to the calcium-binding site of *pf*LamA cause the presence of two sets of resonances which are labeled as *a* and *b* in the data set, respectively. The first set of assignments is derived from a sample in which half of the *pf*LamA molecules have their calcium-binding site filled with Ca^{2+}. The second set of assignments lists assignments of backbone chemical shifts of *pf*LamA in the presence of 10 mM $CaCl_2$; a condition where all *pf*LamA molecules have their calcium-binding site filled with Ca^{2+}. Near-complete (>99%) assignments of chemical shifts of *pf*LamA are obtained.

The assigned ^1H–^{15}N HSQC spectrum of a *pf*LamA sample in which approximately half of the protein molecules have their calcium-binding site filled with Ca^{2+} is shown in Fig. 3. Amides of many amino acid residues that are in proximity to the calcium-binding site cause the presence of two sets of ^1H and ^{15}N NMR signals, as the protein is in slow exchange on the NMR chemical shift timescale between calcium-containing and no calcium-containing conformations (on basis of line shape analysis of the Hε resonance of W64, the rate of exchange between the two conformers is estimated to be approximately 30–46 s^{-1}). Calcium titration experiments provided ^1H–^{15}N HSQC data that clearly reveal which cross peaks are affected by the presence of calcium (data not shown). Hence, in the HSQC spectrum obtained a distinction between *pf*LamA molecules with their calcium-binding site occupied and those in which the binding site does not contain calcium can be made. Some residues in the calcium-binding site of *pf*LamA give rise to NMR signals that are broadened beyond detection, as the corresponding chemical shift differences are smaller than those observed for Hε of W64, while interconversion between the two protein conformers occurs at 30–46 s^{-1}, and thus exchange is intermediate on the chemical shift timescale. These severely broadened, mostly backbone, signals become detectable only after addition of excess calcium (i.e., in presence of approximately 10 mM Ca^{2+}).

Nearly all backbone resonances (i.e., HN, N, Cα, Cβ, and C′) of the calcium-containing form of *pf*LamA (in the presence of approximately 10 mM $CaCl_2$) and of the *pf*LamA conformer with the calcium-binding site unoccupied have been assigned. For the calcium-containing form of the protein, resonances of M34, amide resonances of V35, S196, and E239, and carbonyl resonances of V35 and P133 are not assigned. The intensities of the amide proton signals of V35 and S196 are very weak, which is probably due to fast exchange of these protons with protons of the solvent, whereas the amide resonances of E239 in both *pf*LamA conformers could not be assigned due to overlap with signals of the 25 other glutamates of the protein. For the *pf*LamA conformer with the calcium-binding

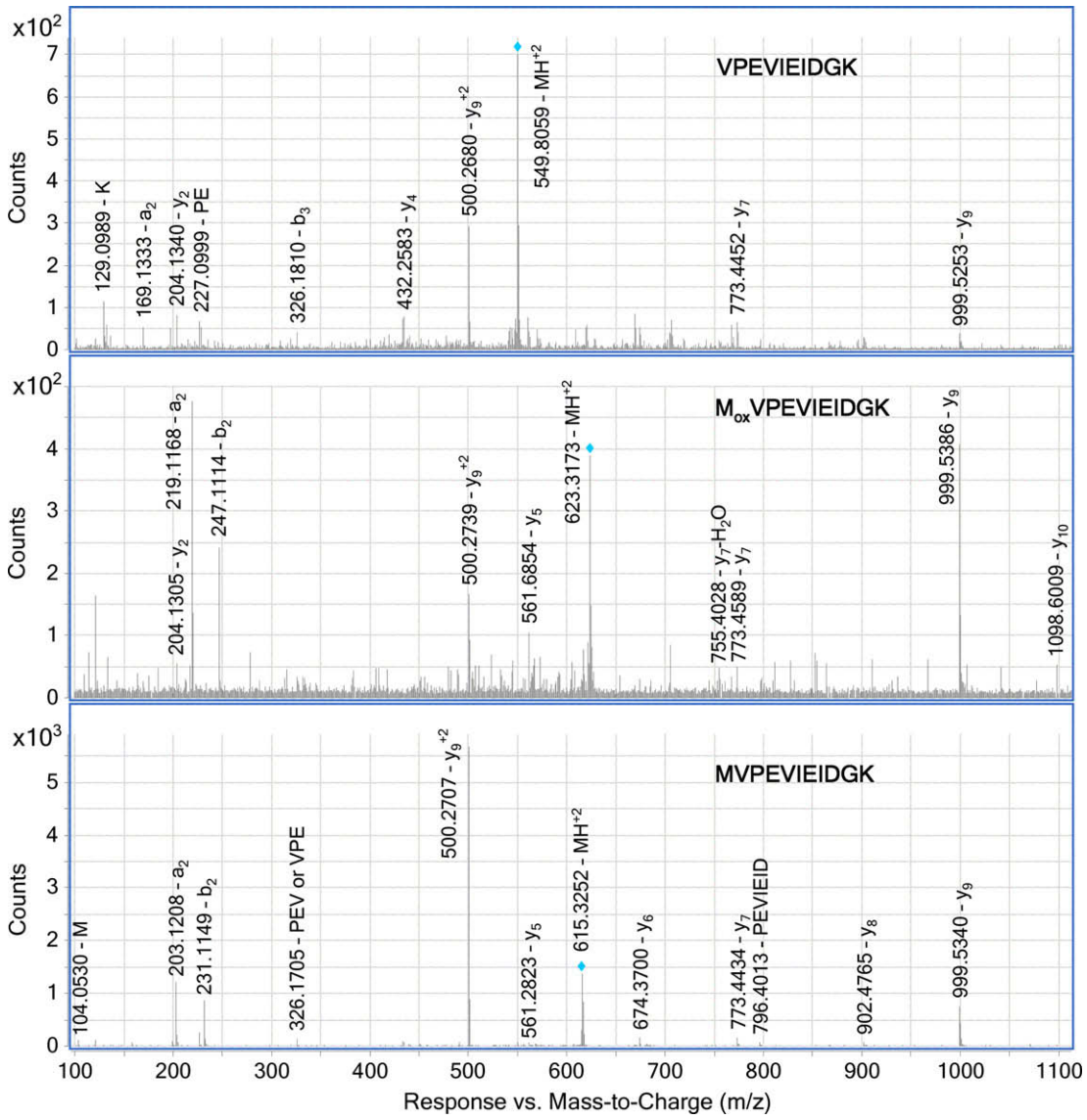

Fig. 2. MS/MS spectral peak assignments of *pf*LamA's, trypsin-digested, N-terminal peptide fragment. Analysis of the spectra shows the presence of three populations of *pf*LamA molecules: a population in which M34 is missing from the protein sequence (top panel), a population in which M34 is oxidized (middle panel), and a population in which M34 is non-oxidized (bottom panel). Blue diamonds indicate the precursor ion location. (For interpretation of the references to color in this figure legend, the reader is referred to the web version of this article.)

site unoccupied, the backbone amides of E53, S57, E89, N96, S196, and A276 could not be assigned due to exchange broadening.

The large majority of resonances of the side chains of the *pf*LamA molecules that contain no calcium have identical chemical shifts, within the limited digital resolution of 3D NMR spectra, compared to the corresponding resonances of the calcium-containing form of the protein. Only a few exceptions exist, see e.g. resonances of the side-chain of W64 (Fig. 3). These exceptions are reported in the deposited chemical shift list.

Virtually all proton and carbon resonances of amino acid side chains of *pf*LamA (Hβ-Hε/Cβ-Cε) are assigned using an HCCH-TOCSY experiment. Side-chain assignments are not obtained for M34 and for the Hε/Cε resonances of the other methionines. Resonances of side-chain amide protons of N90, N96, N112, N167, N263, and N273 are not assigned because they are severely broadened as a result of the unfavorable rate of rotation around the C–N amide bond at 62 °C, and due to exchange of these amide protons with protons of the solvent. The protein contains 6 histidines and 41 aromatic residues. Only the Hε1, Nε1, and Hδ1 resonances of the 11 tryptophan residues of *pf*LamA could be unambiguously assigned.

Residues affected upon calcium binding

Based on the crystal structure of *pf*LamA, calcium is ligated to the carbonyl oxygen atoms of E53, G97, and D287, the carboxyl side-chain oxygens of E55 and D287, and to two water molecules [7].

In case of several proteins, upon Ca^{2+} binding large ^{15}N chemical shift changes have been observed for backbone nitrogens that are covalently bonded to the carbonyls that coordinate a calcium ion (see e.g. [22]). In contrast, the ^{1}H–^{15}N HSQC spectra of *pf*LamA presented here demonstrate that upon binding of calcium chemical shift changes are relatively small. Thus, binding of calcium causes only minor conformational modifications of the *pf*LamA protein. Chemical shifts of the backbone amides of the following 23 residues are affected: W50, H51, D52, F54, E55, G56, S57, E58, N60, W64, Y93, V95, G97, T98, L99, V100, E138, R140, I141, F219, V286, V289, and R290. In addition, cross peaks of the backbone amides of E53 and D287, involved in the direct coordination of calcium, are severely broadened and only visible in the ^{15}N–^{1}H HSQC spectrum of the calcium-containing form of *pf*LamA. The

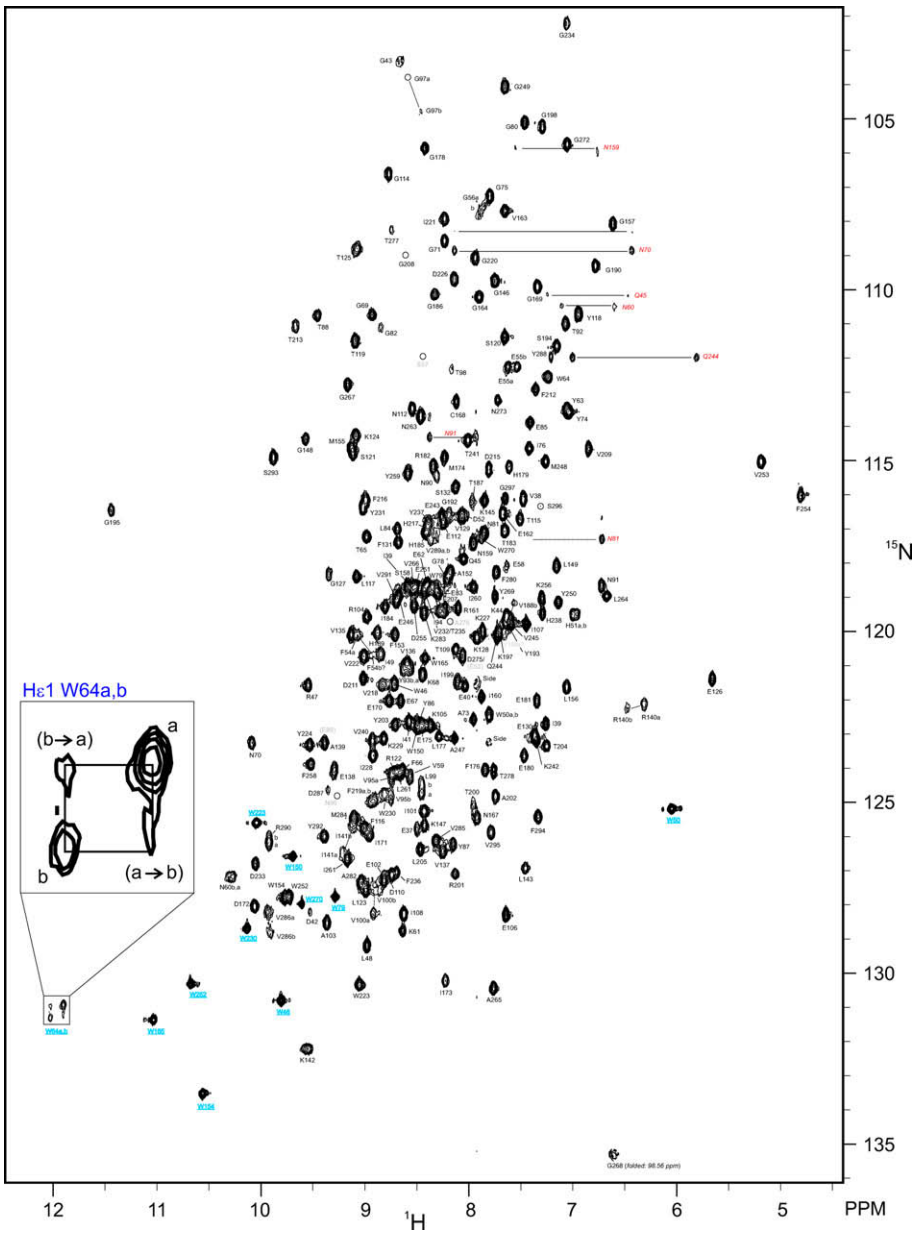

Fig. 3. Gradient-enhanced 500 MHz ^{1}H–^{15}N HSQC spectrum of 264-residue ^{13}C–^{15}N-labeled *pf*LamA at 62 °C. About half of the *pf*LamA molecules have their calcium-binding site filled. As exchange between calcium-containing and non calcium-containing forms of *pf*LamA occurs with a rate of 30–46 s^{-1} many residues that are in the immediate vicinity of the calcium-binding site give rise to a double set of resonances (exchange for these residues is slow on the NMR chemical shift timescale). Cross peaks that have been labeled *a* represent the calcium-containing form, whereas cross peaks that have been labeled *b* arise from the non calcium-containing form of *pf*LamA. Labels highlighted in blue indicate cross peaks from tryptophan side chains. The magnified inset shows four cross peaks arising from Hε/Nε of the indole of W64. Two of these cross peaks arise due to conformational exchange on the millisecond timescale between conformers *a* and *b*. Horizontal lines connect side-chain NH_2 resonances of asparagines and glutamine residues, respectively. Side-chain connectivities of arginines and lysines that could not be assigned are labeled as "*side*". This figure is available in high-resolution (see Supplementary Fig. 1).

corresponding cross peaks of the calcium-free conformer are broadened beyond detection. Most of these 25 affected residues reside in the immediate vicinity of the Ca^{2+} binding site, which is remote from the active site of *pf*LamA (Fig. 1B). Half of these residues (i.e., W50, H51, D52, T93, V95, L99, V100, E138, R140, I141, F219, V286, V289, and R290) are part of the beta sheet frontal to the calcium-binding site and are not in direct contact with the Ca^{2+} ion. The chemical shift changes of these residues upon calcium binding are most likely due to small structural alterations in the hydrogen-bonding network between adjacent anti-parallel beta strands.

Residues W64, G97, V95, V100, R140, I141, V286, and D287 are most affected upon Ca^{2+} binding, as deduced from the size of the magnitude of the corresponding chemical shift changes (data not shown). The crystal structure of *pf*LamA shows that its N-terminus resides in the vicinity of the bound calcium ion. However, our NMR data show that the N-terminus is flexible (i.e., no long-range NOE's are observed and chemical shifts are close to random coil values). In addition, upon calcium binding no chemical shift changes are observed for the N-terminal residues.

Calcium does not significantly increase the stability of pfLamA against thermal unfolding

DSC analysis reveals that *pf*LamA in which approximately half the protein molecules have their calcium-binding site occupied with calcium denatures at 109.3 ± 0.6 °C (Fig. 4). Addition of

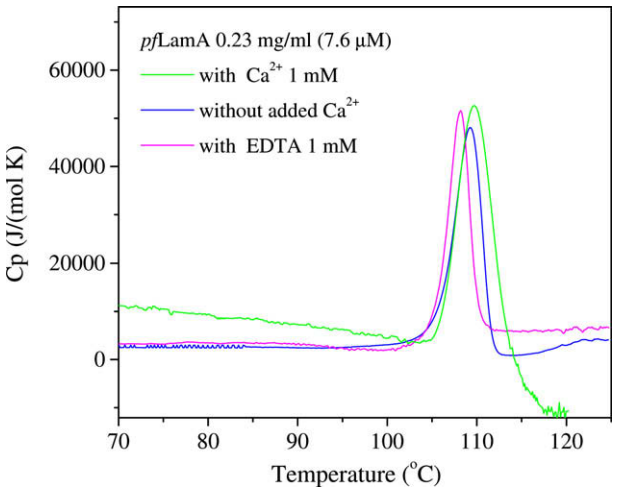

Fig. 4. Temperature-dependence of the heat capacity of *pf*LamA. The protein (7.6 μM) is in 10 mM sodium phosphate, pH 7.0, either without excess Ca^{2+} (red line, denaturation temperature, T_d = 109.3 ± 0.6 °C) or with 1 mM excess Ca^{2+} (green line, denaturation temperature, T_d = 109.7 ± 0.4 °C), or in presence of 1 mM EDTA (blue line, T_d = 108.1 ± 0.5 °C). Graphs are vertically shifted for the purpose of mutual comparison. The scan rate is 30 °C/h.

1 mM Ca^{2+} leads to no significant increase in denaturation temperature, T_d, of *pf*LamA, as now T_d is 109.7 ± 0.4 °C. Calcium-depleted *pf*LamA, generated through addition of 1 mM EDTA, gives a reproducible thermal transition and its T_d is 108.1 ± 0.5 °C. Thus, removal of Ca^{2+} does alter the T_d of *pf*LamA only slightly, implying that Ca^{2+} is not important for the stabilization of the enzyme against global unfolding. However, bound calcium may play a role in protecting the protein against thermal-induced loss of enzymatic activity [3], which may occur before global unfolding of a protein. This loss in activity is likely due to local unfolding processes that occur at temperatures below the denaturation temperature of *pf*LamA.

Acknowledgments

NMR spectra were recorded in the Netherlands at the Utrecht Facility for High-Resolution NMR and at the Wageningen NMR Centre. This project was financially supported by grants from the Graduate School VLAG (Advanced studies on Food Technology, Agrobiotechnology, Nutrition and Health Sciences) of Wageningen University and The Dutch Separation Technology Institute (DSTI). DSC data were collected using the Laboratory of Food Chemistry facilities of Wageningen University and using the Biophysical Instrumentation Facilities of MIT. The Center for Environmental Health Sciences (CEHS; Grant No. NIEHS ES002109) at MIT provided facilities for mass spectrometric analysis.

Appendix A. Supplementary data

Supplementary data associated with this article can be found, in the online version, at doi:10.1016/j.bbrc.2009.11.065.

References

[1] G. Fiala, K.O. Stetter, *Pyrococcus furiosus* sp. *nov*. represents a novel genus of marine heterotrophic archaebacteria growing optimally at 100 °C, Arch. Microbiol. 145 (1986) 56–61.
[2] L.D. Unsworth, J. Van der Oost, S. Koutsopoulos, Hyperthermophilic enzymes – stability, activity and implementation strategies for high temperature applications, FEBS J. 274 (2007) 4044–4056.
[3] Y. Gueguen, W.G. Voorhorst, J. van der Oost, W.M. de Vos, Molecular and biochemical characterization of an endo-beta-1, 3-glucanase of the hyperthermophilic archaeon *Pyrococcus furiosus*, J. Biol. Chem. 272 (1997) 31258–31264.
[4] B.L. Cantarel, P.M. Coutinho, C. Rancurel, T. Bernard, V. Lombard, B. Henrissat, The carbohydrate-active enzymes database (CAZy): an expert resource for glycogenomics, Nucleic Acids Res. 37 (2009) D233–D238.
[5] S. Koutsopoulos, J. Van der Oost, W. Norde, Temperature-dependent structural and functional features of a hyperthermostable enzyme using elastic neutron scattering, Proteins 61 (2005) 377–384.
[6] S. Koutsopoulos, J. Van der Oost, W. Norde, Conformational studies of a hyperthermostable enzyme, FEBS J. 272 (2005) 5484–5496.
[7] A. Ilari, A. Fiorillo, S. Angelaccio, R. Florio, R. Chiaraluce, J. van der Oost, V. Consalvi, Crystal structure of a family 16 endoglucanase from the hyperthermophile *Pyrococcus furiosus* – structural basis of substrate recognition, FEBS J. 276 (2009) 1048–1058.
[8] N. Planas, Bacterial 1,3-1,4-beta-glucanases: structure, function and protein engineering, Biochim. Biophys. Acta 1543 (2000) 361–382.
[9] R. Chiaraluce, G. Gianese, S. Angelaccio, R. Florio, J.F.T. van Lieshout, J. van der Oost, V. Consalvi, Calcium-induced tertiary structure modifications of endo-β-1,3-glucanase from *Pyrococcus furiosus* in 7.9 M guanidinium chloride, Biochem. J. 386 (2005) 515–524.
[10] C. Vetriani, D.L. Maeder, N. Tolliday, K.S.P. Yip, T.J. Stillman, K.L. Britton, D.W. Rice, H.H. Klump, F.T. Robb, Protein thermostability above 100 °C: a key role for ionic interactions, Proc. Natl. Acad. Sci USA 95 (21) (1998) 12300–12305.
[11] Q. Hua, I.S. Dementieva, M.A. Walsh, K. Hallenga, M.A. Weiss, A. Joachimiak, A thermophilic mini-chaperonin contains a conserved polypeptide-binding surface: combined crystallographic and NMR studies of the GroEL apical domain with implications for substrate interactions, J. Mol. Biol. 306 (2001) 513–525.
[12] J. Hasegawa, T. Yoshida, T. Yamazaki, Y. Sambongi, Y. Yu, Y. Igarashi, T. Kodama, K. Yamazaki, Y. Kyogoku, Y. Kobayashi, Solution structure of thermostable cytochrome c-552 from *Hydrogenobacter thermophilus* determined by 1H-NMR spectroscopy, Biochemistry 37 (1998) 9641–9649.
[13] L. Vakonakis, J.C. Sun, T.F. Wu, A. Holzenburg, S.S. Golden, A.C. LiWang, NMR structure of the KaiC-interacting C-terminal domain of KaiA, a circadian clock protein: implications for KaiA–KaiC interaction, Proc. Natl. Acad. Sci USA 101 (2004) 1479–1484.
[14] A. Jung, C. Bamann, W. Kremer, H.R. Kalbitzer, E. Brunner, High-temperature solution NMR structure of TmCsp, Protein Sci. 13 (2004) 342–350.
[15] M. Leone, P. Di Lello, O. Ohlenschlager, E.M. Pedone, S. Bartolucci, M. Rossi, B. Di Blasio, C. Pedone, M. Saviano, C. Isernia, R. Fattorusso, Solution structure and backbone dynamics of the K18G/R82E *Alicyclobacillus acidocaldarius* thioredoxin mutant: a molecular analysis of its reduced thermal stability, Biochemistry 43 (2004) 6043–6058.
[16] S. Koutsopoulos, Kinetic study on the crystal growth of hydroxyapatite, Langmuir 17 (2001) 8092–8097.
[17] H. McDowel, T.M. Gregory, W.E. Brown, Solubility of $Ca_5(PO_4)_3OH$ in system $Ca(OH)_2$–H_3PO_4–H_2O at 5-degrees-C, 15-degrees-C, 25-degrees-C and 37-degrees-C, J. Res. Natl. Bur. Stand. 81A (1977) 273–281.
[18] E.C. Moreno, W.E. Brown, G. Osborn, Solubility of dicalcium phosphate dihydrate in aqueous systems, Soil Sci. Soc. Am. J. 24 (1960) 94–98.
[19] T.M. Gregory, E.C. Moreno, J.M. Patel, W.E. Brown, Solubility of beta-$Ca_3(PO_4)_2$ in system $Ca(OH)_2$–H_3 PO_4–H_2O at 5, 15, 25, and 37 degrees C, J. Res. Natl. Bur. Stand. 78A (1974) 667.
[20] R.W. Marshall, Complex formation, crystal growth and dissolution in calcium phosphate solutions, Ph.D. Thesis, State University of New York at Buffalo, New York, 1970.
[21] A.E. Martell, R.M. Smith, NIST Critically Selected Stability Constants of Metal Complexes Database: Version 5.0; National Institute of Standards and Technology, Gaithersburg, MD, 1998.
[22] R.R. Biekofsky, S.R. Martin, J.P. Browne, P.M. Bayley, J. Feeney, Ca^{2+} coordination to backbone carbonyl oxygen atoms in calmodulin and other EF-hand proteins: ^{15}N chemical shifts as probes for monitoring individual-site Ca^{2+} coordination, Biochemistry 37 (1998) 7617–7629.